

1 **GreenSynthesis of Manganese Oxide Nanoparticles Using Basil Extract for**
2 **Biocompatibility and Therapeutic Targeting of Metribuzin Poisoned Heart and**
3 **Lung Tissues in *Wistar* Rats**

4
5 **Islam Boulaares^{1,2}, Samir Derouiche^{1,2*}, Sara Chetehouna¹ and Janetta Niemann³,**

6 ¹ Department of Cellular and Molecular Biology, Faculty of Natural Sciences and Life, University of El-
7 Oued, El-Oued 39000, Algeria

8 ² Laboratory of Biodiversity and Application of Biotechnology in the Agricultural Field, Faculty of
9 Natural Sciences and Life, University of El-Oued, El-Oued 39000, Algeria

10 ³ Department of Genetics and Plant Breeding, Poznań University of Life Sciences, Dojazd 11, 60-632
11 Poznań, Poland

12 **Corresponding author:**

13 Samir Derouiche

14 Department of Cellular and Molecular Biology, Faculty of Natural Sciences and Life, University of El-
15 Oued, El-Oued 39000, Algeria

16 dersamebio@gmail.com

17
18
19
20 **Abstract**

21 Manganese oxide nanoparticles have garnered interest for use in a variety of fields, such as
22 biomedical applications, including cancer theranostics and drug delivery. This work aimed to
23 investigate the potential therapeutic and preventative benefits of green-produced MnO NPs made
24 from basil extract against metribuzin-induced oxidative stress, metabolic toxicity, inflammation, and
25 histological changes in the lungs and heart. Green synthesis of MnO NPs using basil extract was
26 done. The shape and size distribution of the MnO nanoparticles were analyzed using TEM and SEM.
27 18 male albino Wistar rats were divided into three groups (n = 6), which consisted of a control group,

28 a metribuzin-treated group, and a MnO NPs-treated group. The objective of this study was to
29 determine the increase in mass for each organ and to evaluate the oxidative stress status by measuring
30 the levels of SOD, GPx, GSTs, CAT, GSH, and MDA in the lungs and heart tissues. Additionally,
31 the tissue histology of the organs was examined, and various biochemical parameters (GOT, LDH, and
32 CPK) and inflammation markers (WBC, Lymph, Mid, and Gran) were estimated. The green synthesis
33 of MnO NPs is shown by the gradual shift in color from golden yellow to dark brown. . The
34 morphological characteristics and particle size distribution of the MnO NPs were identified using
35 TEM and SEM. The analyses revealed that the MnO NPs were uniformly spherical in shape, with an
36 average particle size of 6.52 ± 0.88 nm. Results of the *in vivo* rats' study showed that treatment with
37 metribuzin induced growth in the weight of organs, oxidative stress, biochemical toxicity,
38 inflammation, and histological changes in the lungs and heart, as well as a significant amelioration of
39 MnO NPs against the toxic effects induced by metribuzin by reversing all of the previous parameters.
40 In conclusion, the results of the *in vivo* investigation showed that rats given metribuzin herbicide
41 suffered from organs weight gain, oxidative stress, biochemical toxicity, inflammation, and
42 histological alterations in their lungs and heart. Additionally, MnO NPs show effective therapeutic
43 and preventive actions against lungs and heart damage caused by metribuzin. Basil extract's
44 phytochemical components enhance MnO NP biocompatibility, reduce toxicity, and provide
45 antioxidant and anti-inflammatory properties, making them safe and therapeutic for biomedical
46 applications.

47
48 **Keywords:** MnO NPs; Metribuzin; Oxidative stress; Inflammation; Lungs; Heart.

54 1. Introduction

55 Metribuzin, identified as a 4-amino-6-(1,1-dimethyl)-3-(methylthio)-1,2,4-triazin 5(4H)-one
56 compound categorized as an asymmetric triazine, was officially approved for use in the United States
57 in 1973 specifically for herbicidal utilization (1). Metribuzin is frequently utilized in the cultivation
58 of potatoes, soybeans, peas, tomatoes, and lentils (2). Adverse impacts on humans, fish, and domestic
59 animals have been recorded in relation to its usage (3). Metribuzin, a xenobiotic, explicates the
60 mechanisms of toxicity in the majority of xenobiotics, which are chemical compounds that are

61 foreign to the body and include herbicides and environmental pollutants. These mechanisms include
62 disturbance of the body's overall antioxidant capacity and stimulation of free radical production-
63 induced lipid peroxidation (4).

64 Over the last several years, manganese oxide nanoparticles have garnered interest for use in a
65 variety of fields, such as water treatment, catalysis, and solar cells, as well as in biomedical
66 applications, including biosensors and bioimaging, cancer theranostics, and drug delivery (5).
67 Manganese oxides are a mixed oxide substance that finds extensive application in fields such as
68 electrochemistry, medicine, and catalysis. This is because they are affordable, environmentally
69 benign, occur in diverse forms of manganese, and are abundant in nature (6). Nanoparticles can be
70 created using a variety of methods, such as chemical, physical, and biological ones (7). Green
71 synthesis of nanoparticles has been developed to lower costs, minimize pollution, improve the
72 environment, and protect human health by using plant extracts instead of industrial chemical
73 components to reduce metal ions (8). Phytochemicals found in medicinal plants can be used to create
74 biocompatible, affordable, and renewable green nanoparticles (9). The purpose of the current study
75 was to examine the therapeutic and preventive effects of MnO NPs greenly produced using basil
76 extract against the growth in weight of organs, oxidative stress, biochemical toxicity, inflammation,
77 and histological alterations caused by metribuzin exposure in the lungs and heart.

79 **2. Materials and Methods:**

80 *2.1.Plant Materials Collection*

81 Professor Youssef Hallis identified the plant used in this experiment. The basil was harvested in
82 August 2022 from the El-Oued (Guemar) region of Algeria. The basil leaves were cleaned, dried,
83 and stored at room temperature away from direct sunlight. A mechanical grinder was then used to
84 grind the dry leaves into a fine powder. *Ocimum basilicum* L. powder is stored at room
85 temperature in airtight containers until the experiment starts.

86 *2.2.Aqueous Extract Preparation*

87 Ten g of dried leaves were boiled for two hours at 50 °C in 100 ml of distilled water to make basil
88 aqueous extract. The extract was macerated for 24 hours at room temperature then filtered
89 through Whatman filter paper. Following that, a rotary evaporator was used to evaporate it, and an
90 oven was used to dry it.

91 *2.3.Compounds Analysis*

92 The aqueous plant extract was subjected to a thorough examination using a standardized
93 methodology to identify the presence of different phytochemicals.

94 2.4. Green Synthesis of MnO NPs

95 Manganese oxide nanoparticles were created using a green synthesis approach mediated by
96 *Ocimum basilicum* L. leaf extract, but with minor changes based on the methodology of Saod *et al.*
97 (10). This procedure entailed the amalgamation of the aqueous extract of basil with a manganese (II)
98 chloride ($\text{MnCl}_2 \cdot 4\text{H}_2\text{O}$) solution. To attain a pH of 8, sodium hydroxide (NaOH) solution was
99 incrementally added to the mixture while maintaining continuous stirring, which facilitated the
100 generation of diminutive particles. The resultant solution was subsequently subjected to magnetic
101 stirring at a temperature of 65 °C for a duration of 6 hours, during which a colorimetric transition
102 from golden yellow to dark brown occurred, indicative of the successful biosynthesis of MnO NPs.
103 Following this, the mixture was centrifuged at 5000 rpm for 20 minutes, after which the supernatant
104 was discarded. The resulting precipitate was subjected to three washing cycles utilizing distilled
105 water and ethanol prior to being desiccated to yield the final product.

106 2.5. Characterization of MnO NPs

107 Transmission electron microscopy (TEM) and scanning electron microscopy (SEM) analyses
108 were conducted to evaluate the morphological characteristics and particle size distribution of the
109 manganese oxide nanoparticles (MnO NPs) greenly synthesized using basil extract.

110 2.6. Animal Care and Experimental Design:

111 In our investigation, 18 male Wistar rats, weighing 206 ± 9.02 g, were used. The rats were 08
112 weeks old when they were obtained from the Pasteur Institute in Algiers. The Faculty of Natural and
113 Life Sciences at Echahid University Hamma Lakhdar-El-Oued's animal husbandry laboratory is
114 where these animals were grown. The rats had the same living conditions, including a 12-hour
115 photoperiod of light and darkness and room temperature, and were kept in plastic cages with metal
116 mesh coverings. They were also given a standard diet and free access to food and water. Over the
117 course of 08 weeks, the experiment was conducted.

118 Following a two-week adaptation period, the animals were divided up into 03 experimental
119 groups, each with six animals:

120 **Group 1 (Control):** Healthy rats received water and administered intraperitoneally with
121 physiological saline solution.

122 **Group 2 (MTZ):** Rats exposed to metribuzin and administered intraperitoneally with
123 physiological saline solution.

124 **Group 3 (MnO NPs):** Rats exposed to metribuzin and administered intraperitoneally with
125 MnO NPs (one dose/day, 05 mg/kg).

126 Oral dose of metribuzin in drinking water (220 mg/kg) was used to cause intoxication for eight
127 weeks. The rats received four weeks of treatment with MnO NPs. We injected groups 1 and 2 with
128 physiological saline solution to subject rats to the same experimental conditions.

129 *2.7. Sacrifice, Blood Sampling and Tissues Collection*

130 Following an 8-week treatment period and a 16-hour fast, the rats were sacrificed by inhaling a
131 small amount of chloroform (94%). During the animal sacrifice process, blood samples have been
132 placed into dry tubes to obtain serum by centrifugation for 10 minutes at 3000 tour/min, which was
133 used to assess GOT, LDH, and CPK activity, and into EDTA tubes for leukocyte line studies. the
134 lungs and heart were carefully sampled, cleaned, weighted, and kept at -20°C in order to
135 homogenates preparation to measure oxidative stress. In addition, the organs were preserved in 10%
136 formaldehyde for histological examination.

137 *2.8. Biochemical Parameters and Inflammation Markers*

138 The following reference codes, which correspond to commercial kits from Spinreact, represent
139 the enzymatic activity of aminotransferase (GOT), lactate dehydrogenase (LDH), and creatine
140 phosphokinase (CPK): GOT-1001161, LDH-1001260, and CPK-1001217. The hematology
141 autoanalyzer (Sysmex) measures the levels of inflammation markers (WBC, Lymph, Mid, and Gran).

142 *2.9. Tissue Samples Preparation and Lungs and Heart Oxidative Stress Parameters*

143 The procedure used by Boulaares *et al.* was followed to prepare homogenates from lungs and
144 heart tissue. Following Beauchamp and Fridovich (11), Flohe and Gunzler (12), Habig *et al.* (13),
145 Regoli and Principato (14), Weckbecker and Cory (15) and Draper and Hadley (16) methods, the
146 levels of SOD, GPx, GSTs, CAT GSH, and MDA levels were measured, respectively.

147 *2.10. Histopathological Study*

148 Following the rats' sacrifice, the tissues from the lungs and heart were removed and kept in a
149 fixative solution containing 10% formaldehyde until it was time to prepare the slides. The tissues
150 were then washed with toluene, immersed in paraffin, and stained with hematoxylin and eosin after
151 being dehydrated using an increasing series of ethanol. The final slides had been examined under a
152 microscope that had a camera attached, and the computer screen showed the pictures that the camera
153 had taken.

154 *2.11. Statistical Analysis*

155 In order to express the results as either an average \pm ES (standard deviation), the study used the
156 student's t-test for independent samples. Minitab 13.0 software was used to analyze all the data, and a
157 P-value of less than 0.05 was used to assess statistical significance.

158 3.Results

159 3.1.Bioactive Compounds Analysis

160 Phytochemical examination revealed the presence of phenols, flavonoids, catechic tannins,
161 terpenes, saponins, reducing sugars, and alkaloids in *Ocimum basilicum* L. aqueous extract (**Table**
162 **01**).

163 **Table 01:** Bioactive compounds of *Ocimum basilicum* L. aqueous extract.

Bioactive compounds	Basil extract	Test
Phenols	+	Ferric chloride test
Flavonoids	+	Magnesium test
Catechic tannins	+	Ferric chloride test
Terpenes	+	Salkowki's test
Saponins	+	Froth test
Reducing sugars	+	Fehling test
Alkaloids	+	Dragendorff's test

164 3.2.Synthesis and Characterization of MnO NPs

165 The change in color to dark brown from golden yellow over time indicates the green synthesis
166 of MnO NPs through the use of basil extract (**Figure 01**).

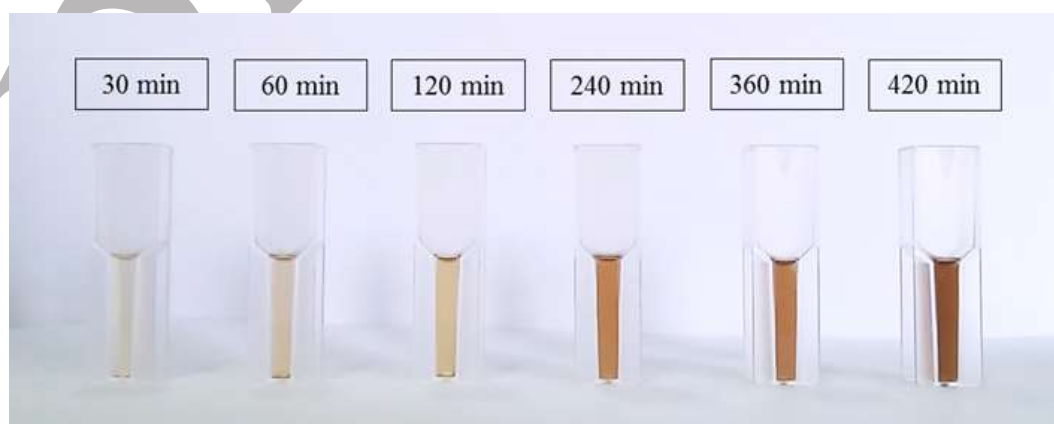


Figure 01: Green synthesis of MnO NPs using *Ocimum basilicum* L. extract at different time.

167 The images from the scanning and transmission electron microscopes (**Figure 02 A/B**) show
 168 that the MnO NPs are uniformly spherical in shape and have a homogeneous dispersity. The MnO
 169 NPs' average particle size was determined to be 6.52 ± 0.88 nm (**Figure 02 C**).

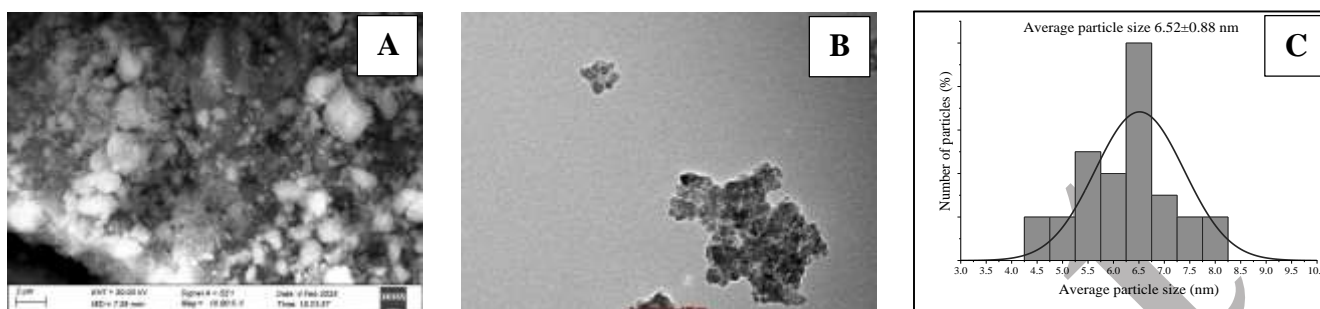


Figure 02: MnO NPs' morphological characteristics based on SEM image (A), TEM image (B) and their diameter (nm) (C).

170 3.3. Relative Lungs and Heart Weight

171 The MTZ group showed a significant rise in relative lung and heart weight when compared to
 172 the control group, but the MnO NPs group showed a significant decrease when compared to the MTZ
 173 group (Table 02).

174 **Table 02:** Relative lungs and heart weight in control and MnO NPs group.

	Control	MTZ	MnO NPs
Lungs	0.665±0.005	2.138±0.503**	0.990±0.110 */###
Heart	0.254±0.003	0.324±0.023 *	0.298±0.004 ***/##

175 Data are expressed as mean ± SD (n=6).

176 * p<0.05, **p<0.01, ***p<0.001: significantly different from control group.

177 #p<0.05, ##p<0.01, ###p<0.001: significantly different from metribuzin exposed group.

178 3.4. Biochemical Parameters

179 The activity levels of GOT, LDH, and CPK showed a significant increase (P<0.05) in the MTZ
 180 group in comparison to the control group, and there was also a partial improvement observed in the
 181 MnO NPs group when contrasted with the MTZ group (**Figure 03**).

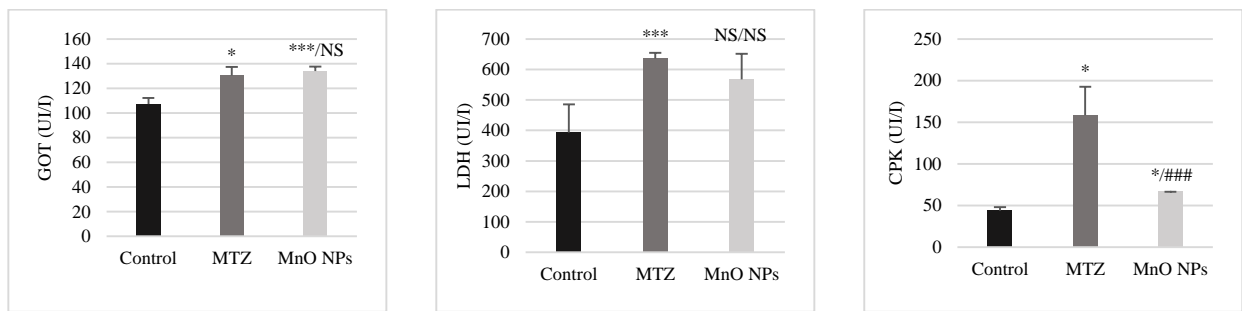


Figure 03: GOT, LDH, and CPK activity in heart in control and MnO NPs group.

182 **3.5. Inflammation Markers**

183 The levels of inflammation markers (WBC, Lymph, Mid, and Gran) in the MTZ group were
 184 found to be significantly higher than those in the control group ($P < 0.05$). On the other hand, there
 185 was a highly significant decrease ($P < 0.001$) in the levels of WBC, Mid and Gran with no significant
 186 change ($P > 0.05$) in the levels of Lymph in the MnO NPs group compared to the MTZ group (**Figure**
 187 **04**).

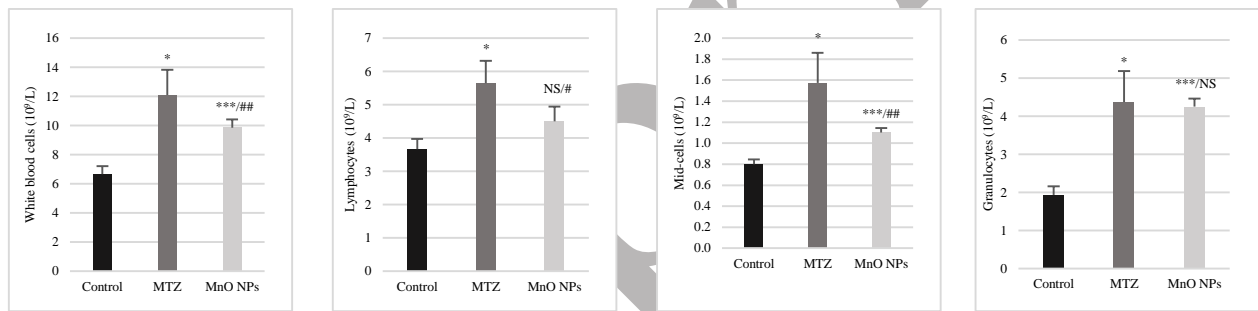


Figure 04: Inflammation markers level in control and MnO NPs group.

188 **3.6. Oxidative Stress Parameters**

189 The results of the enzymatic activity tests indicated that there were no noticeable changes in the
 190 activity of SOD and CAT in the lungs, a significant increase in the activity of GSTs in both the lungs
 191 and heart, and a significant decrease in the activity of GPx in the lungs as well as in the activity of
 192 SOD, GPx, and CAT in the MTZ group compared to the control group. In contrast, there was only a
 193 partial improvement in the activity of these enzymes in the group treated with manganese oxide
 194 nanoparticles (MnO NPs) compared to the MTZ group (**Figure 05**).

195

196

197

198

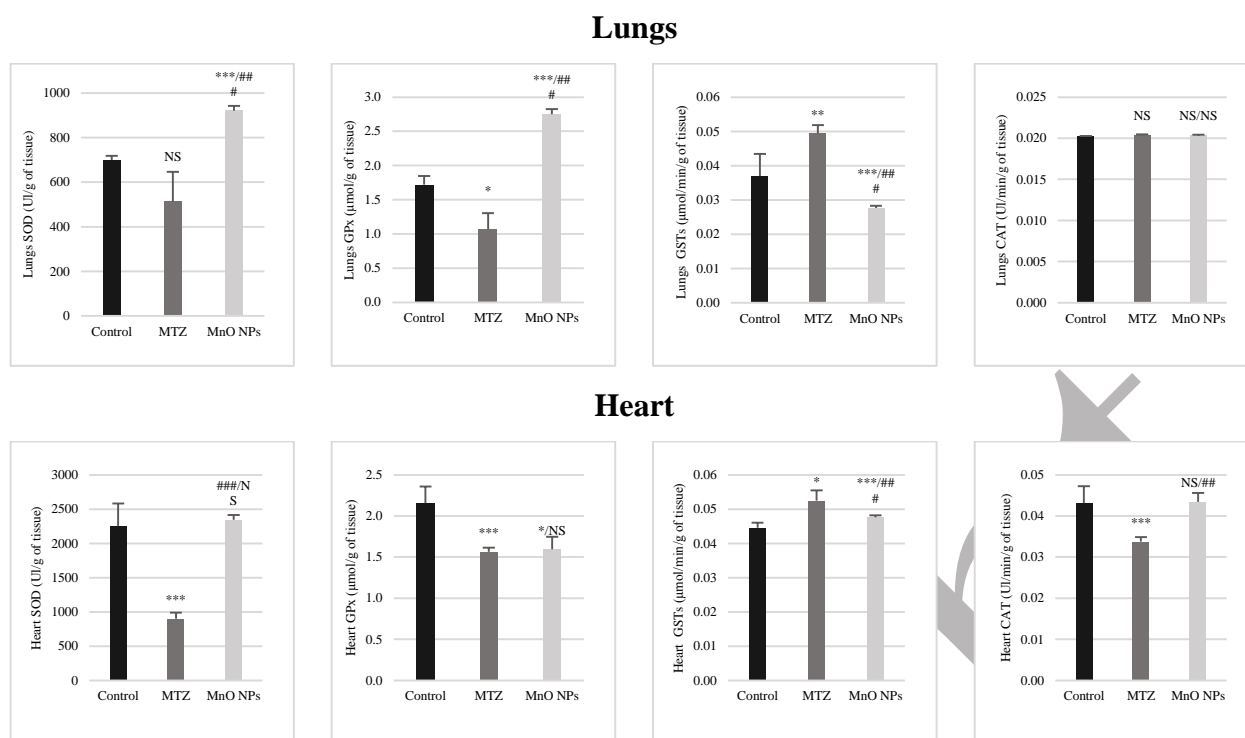


Figure 05: Enzymatic antioxidant activity in lungs and heart in control and MnO NPs group.

199 Our research findings showed a significant decrease in the level of GSH in both the lungs
 200 ($P < 0.01$) and heart ($P < 0.001$) tissues of the MTZ group compared to the control group. Additionally,
 201 there was a very highly significant increase in MDA level in both tissues ($P < 0.001$). However, there
 202 was a remarkable improvement in GSH and MDA levels in the MnO NPs group versus the MTZ
 203 group (Table 03).

204 **Table 03:** GSH and MDA levels in lungs and heart in control and MnO NPs group.

	Control	MTZ	MnO NPs
Lungs			
GSH levels (nmol/g of tissue)	9.377±0.606	4.402±0.897 **	7.946±0.36 */###
MDA levels (nmol/g of tissue)	8.627±0.305	10.088±0.205 ***	9.647±0.105 ***/##
Heart			
GSH levels (nmol/g of tissue)	3.8713±0.0778	2.6428±0.0553 ***	3.058±0.311 */NS
MDA levels (nmol/g of tissue)	17.460±1.64	25.150±0.913 ***	21.920±1.15 */#

205 Data are expressed as mean ± SD (n=6).

206 * p<0.05, **p<0.01, ***p<0.001: significantly different from control group.
 207 #p<0.05, ##p<0.01, ###p<0.001: significantly different from metribuzin exposed group.

208 *3.7.Histopathological Study*

209 The control rat's lung section showed typical histological features, including thin alveolar septa.
 210 In contrast, the MTZ-treated group's lung tissue exhibited several histological changes, such as
 211 thickened interalveolar septa and completely blocked air spaces. These areas displayed evidence of
 212 hemorrhage and inflammatory cell infiltration within the markedly thickened septa. The MnO NPs
 213 group demonstrated partial lung tissue recovery, with some alveoli remaining collapsed while others
 214 were expanded and ruptured. Control rat heart tissues revealed normal myofibrillar structure and cells
 215 under microscopic examination. Conversely, MTZ-treated rat heart tissues showed muscle fiber
 216 abnormalities, including hemorrhage, inflammation, necrosis, and vacuolization of cardiomyocytes.
 217 The MnO NPs group, however, exhibited considerable improvement, with heart tissue morphology
 218 more closely resembling that of the control group (**Figure 06/**Table 04).

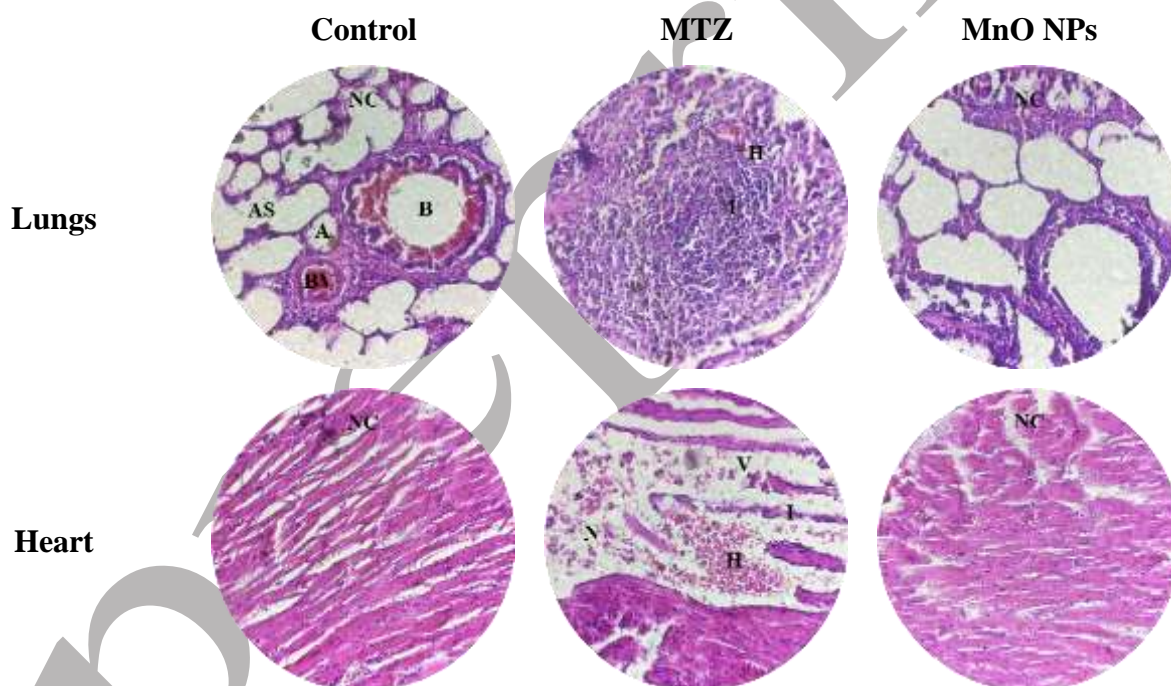


Figure 06: Photomicrographs of lungs and heart section of all experimental groups, stained using hematoxylin and eosin (H&E), shown at 40 x 10 magnification.

Normal cells: **NC**; Hemorrhage: **H**; Inflammation: **I**; Vacuolization: **V**; Necrosis: **N**
 Bronchiole: **B**; Alveolus: **A**; Blood vessels: **BV**; Alveolar sacs: **AS**

219 **Table 04:** Grading of histological alterations in the lungs and heart sections of all experimental
 220 groups.

Parameters	Control	MTZ	MnO NPs
------------	---------	-----	---------

Hemorrhage	Lungs	-	++	-
	Heart	-	+++	-
Inflammation	Lungs	-	+++	-
	Heart	-	++	-
Vacuolization	Lungs	-	-	-
	Heart	-	+++	-
Necrosis	Lungs	-	-	-
	Heart	-	+++	-

221 None (-); Moderate (+); Severe (++); Very severe (+++)

222 4. Discussion

223 This study investigated the therapeutic and preventive benefits of MnO NPs against metribuzin-
224 induced organs weight gain, oxidative stress, biochemical toxicity, inflammation, and histological
225 alterations in the heart and lungs.

226 Our study revealed the presence of phenols, flavonoids, catechic tannins, saponins, reducing
227 sugars, alkaloids, and terpenes in basil aqueous extract. Based on the information from **Nadeem et al.**
228 (17), the current findings are consistent with their results, which indicated the presence of alkaloids,
229 phenols, tannins, flavonoids, terpenoids, steroids, and glycosides in the basil leaf aqueous extract.
230 According to published research, the active substances in medicinal plants called phytochemicals are
231 thought to have pharmacological potential.

232 The solution's hue changes from golden yellow to dark brown in relation to the green
233 synthesis of MnO NPs, indicating the biogenesis of MnO NPs utilizing basil extract. Initially, the
234 optical observation of color modification was used to confirm the plant extract's ability to create
235 nanoparticles (18).

236 The color shift of the metal ion solution, which serves as a visual cue, is necessary for the
237 synthesis of MnO NPs, as **Khan et al.** confirmed (19). The average particle size and shape were
238 investigated using TEM and SEM pictures. The findings showed that the average size of MnO NPs
239 was 6.52 ± 0.88 nm and that they were spherical in shape.

240 Comparing the MTZ group to the control group, there was a significant increase in relative lung
241 and heart weight; whereas, there was a significant decrease in the MnO NPs group when compared to
242 the MTZ group. Changes in the weight of the organs, either in absolute terms or in relation to body
243 weight, are extremely sensitive markers of early toxicity, especially when under strictly regulated
244 circumstances, like in an experiment (20). Experimental rats who received subacute metribuzin may
245 have experienced negative effects, as evidenced by the significant increase in the absolute and
246 relative weight of several vital organs (3). It has been demonstrated that plant extract-mediated

247 synthesis can decrease toxicity while improving the biological properties (bioavailability,
248 biocompatibility, cell internalization, and antioxidant activity) of metal and metal oxide nanoparticles
249 (5). Because MnO NPs are less harmful, they have become more important in the synthesis and
250 production processes, which eliminates the metribuzin effect responsible for lungs and heart
251 hypertrophy.

252 When comparing the MTZ group to the control group, the activity levels of GOT, LDH, and
253 CPK significantly increased, and the MnO NPs group showed partial improvement in comparison to
254 the MTZ group. The three primary cardiac enzymes that are measured are GOT, LDH, and CPK. The
255 enzymes present in cardiomyocytes can be found in the blood, and when cardiac cells suffer
256 inflammation (myocarditis) or necrosis (myocardial infarction) due to a variety of reasons, the
257 activity (content) of these enzymes increases (21). The outcomes observed indicate that manganese
258 oxide nanoparticles could potentially have cardioprotective effects by regulating metribuzin-induced
259 oxidative stress and inflammation, which are the principal causes of cell damage and the release of
260 their contents into the blood.

261 In comparison to the control group, the MTZ group exhibited noticeably higher levels of
262 inflammatory markers. On the other hand, the therapy group showed a significant decrease in
263 inflammatory marker levels as compared to the MTZ group. One important organ to focus on when
264 exposed to pesticides is the immune system (22). The capacity of pesticides to either promote or
265 inhibit lymphocyte proliferation and cytokine synthesis, in addition to inducing genetic injury and
266 chromosomal irregularities in cultured lymphocytes, has been proposed as plausible mechanisms
267 underlying their adverse effects on the immune system (22). The large surface area to volume ratio of
268 these entities allows them to possess high surface reactivity, which in turn facilitates their interaction
269 with biological membranes and promotes their physical transport within the membrane (10).
270 Nanoparticles exhibit improved penetration in epithelial and inflammatory cells, which contributes to
271 their superior effectiveness and longer persistence in treatment. Additionally, they exhibit better
272 targeting of specific sites, such as inflammatory cells or tissues (23). Inhibiting pro-inflammatory
273 cytokines is a crucial process, as these cytokines enhance immune responses and are targeted by the
274 vast majority of nanoparticles (23).

275 The evaluation of oxidative stress biomarkers (SOD, GPx, GSTs, CAT, GSH, and MDA) in the
276 pulmonary and cardiac tissues of male rats revealed that MTZ induces oxidative stress. Concurrently,
277 a significant amelioration was observed in the MnO NPs group in contrast to those in the MTZ
278 group. The antioxidant defense mechanisms, including glutathione (GSH), catalase (CAT),
279 glutathione peroxidase (GST), and superoxide dismutase (SOD), can be inhibited by xenobiotics,
280 which cause the overproduction of untimely and excessive free radicals. This leads to the damage of
281 macromolecules, including DNA (4). Certain pesticides have the potential to induce a rise in reactive

282 oxygen species (ROS) generation, thus resulting in oxidative stress in unintended organisms (3).
283 Metal oxide nanoparticles (NPs), specifically manganese dioxide, can effectively replicate the
284 functions of antioxidant enzymes by catalyzing the breakdown of superoxide anions and hydrogen
285 peroxide (7).

286 The observed increase in organ mass, oxidative stress levels, biochemical toxicity, and inflammatory
287 responses documented in the present investigation were substantiated through histopathological
288 analyses of pulmonary and cardiac tissues. Control rats displayed normal histological features in their
289 pulmonary and cardiac tissues upon examination. In contrast, the MTZ-treated group's lungs and
290 heart samples showed various structural changes. Interestingly, the MnO NPs group exhibited
291 considerable enhancement, with their lung tissue structure closely resembling that of the control
292 group. There exists indirect corroborative evidence that associates pesticide exposure with specific
293 chronic health conditions, including respiratory ailments, notably chronic obstructive pulmonary
294 disease, as well as cardiovascular disorders (2). Research involving animal models has indicated that
295 metribuzin may induce deleterious health consequences, such as alterations in tissue histology (4).
296 Moreover, individual pesticides have been documented to elicit cellular toxicity via oxidant-mediated
297 mechanisms, which encompass both programmed and unprogrammed cell death, lipid membrane
298 damage, metabolic disruption, modification of diverse signaling pathways, or alteration of tight
299 junction integrity (24). This elucidates the varied histological alterations detected in the tissue
300 specimens from the MTZ-exposed group. The amelioration observed in all aforementioned
301 parameters is substantiated by the findings derived from the histological evaluations of the tissue
302 sections. The inverse of the aberrant ROS generation process, MnO₂ NPs can consume excess H₂O₂
303 in situ and convert it to O₂. Additionally, MnO₂ particles can control the degree of inflammation by
304 affecting the expression of genes that produce cytokines. MnO₂ gradually breaks down during this
305 process to produce Mn²⁺, which is expelled with bodily fluids and aids in the return of the body's
306 internal environment to its ideal state (25). We suggest that the phytochemical components of the
307 basil extract used in the green synthesis of MnO NPs play a crucial role in enhancing their
308 biocompatibility by acting as natural reducing, capping, and stabilizing agents, which help produce
309 uniformly sized and shaped nanoparticles. These plant-derived compounds reduce toxicity by
310 eliminating the need for harsh chemicals and create a bio-friendly surface that improves cellular
311 interactions and uptake. Additionally, functional groups from phytochemicals enhance biological
312 compatibility, while their antioxidant and anti-inflammatory properties further contribute to the
313 safety and therapeutic value of MnO NPs, making them well-suited for biomedical applications.

314

315

316

317 **Acknowledgment**

318 We thank the Faculty of Natural and Life Science laboratory staff of El-Oued University, Algeria, for
319 their basic instruction, which was essential to the successful execution of this study.

320

321 **Authors' Contribution**

322 Study concept and design: I.B.

323 Acquisition of data: I.B., S.C.

324 Analysis and interpretation of data: I.B., S.D.

325 Drafting of the manuscript: I.B.

326 Critical revision of the manuscript for important intellectual content: S.D., J.N.

327 Statistical analysis: I.B., S.D.

328 Administrative, technical, and material support: I.B., S.C.

329 Study supervision: S.D., J.N.

330 All authors have read and agreed to publish version of the manuscript.

331

332 **Ethics**

333 We hereby declare all ethical standards have been respected in preparation of the submitted article.

334 **Conflict of Interest**

335 The authors declare no competing interests.

336 **Data Availability**

337 The data that support the findings of this study are available on request from the corresponding
338 author.

339

340 **Reference**

341

- 342 1. Boulaares I, Derouiche S. Review of Metribuzin Pollution and Its Impact on Oxidative Stress in
343 Cardiovascular Diseases. *Pharma Sci Analytical Res J*. 2024; 6(4): 180103.
- 344 2. Derouiche S, Rezzag Mohcen OS, Serouti A. Triazinone herbicide metribuzin induced acute liver
345 injury: A study of animal model. *J Acute Dis*. 2018;7(4):152-7. doi:10.4103/2221-6189.241016.
- 346 3. Kadeche L, Bouroгаа E, Boumendjel A, et al. Quercetin attenuates metribuzin-induced
347 biochemical and hematological toxicity in adult rats. *Int J Pharm Sci Rev Res*. 2016;40(1):38-46 .

- 348 4. Derouiche S, Rezzag Mohcem OS, Serouti A. The effect of herbicide metribuzin on environment
349 and human: A systematic review. J Pharm Biosci. 2020;8(4):10-5.
350 doi:10.20510/ukjpb/8/i4/1593522789
- 351 5. Alsaleh NB, Aljarbou AM, Assal ME, et al. Synthesis, Characterization, and Toxicity Assessment
352 of Zinc Oxide-Doped Manganese Oxide Nanoparticles in a Macrophage Model. Pharmaceuticals.
353 2024;17(2):168. doi:10.3390/ph17020168
- 354 6. Shaik MR, Syed R, Adil SF, et al. Mn₃O₄ nanoparticles: Synthesis, characterization and their
355 antimicrobial and anticancer activity against A549 and MCF-7 cell lines. Saudi J Biol Sci.
356 2021;28(2):1196-202. doi:10.1016/j.sjbs.2020.11.087
- 357 7. Augustine R, Hasan A. Multimodal applications of phytonanoparticles. Phytonanotechnology:
358 Elsevier; 2020. p. 195-219.
- 359 8. Derouiche S, Guemari IY, Boulaares I. Characterization and acute toxicity evaluation of the MgO
360 Nanoparticles Synthesized from Aqueous Leaf Extract of *Ocimum basilicum* L. Alger J
361 Biosciences. 2020;1(1):1-6. doi:10.5281/zenodo4041021.
- 362 9. Thatyana M, Dube NP, Kemboi D, Manicum A-LE, Mokgalaka-Fleischmann NS, Tembu JV.
363 Advances in Phytonanotechnology: A Plant-Mediated Green Synthesis of Metal Nanoparticles
364 Using *Phyllanthus* Plant Extracts and Their Antimicrobial and Anticancer Applications.
365 Nanomaterials. 2023;13(19):2616. doi:10.3390/nano13192616
- 366 10. Saod WM, Hamid LL, Alaallah NJ, Ramizy A. Biosynthesis and antibacterial activity of
367 manganese oxide nanoparticles prepared by green tea extract. Biotechnol Rep. 2022;34:e00729.
368 doi:10.1016/j.btre.2022.e00729
- 369 11. Beauchamp C, Fridovich I. Superoxide dismutase: improved assays and an assay applicable to
370 acrylamide gels. Anal Biochem. 1971;44(1):276-87. doi:10.1016/0003-2697(71)90370-8
- 371 12. Flohé L, Günzler WA. [12] Assays of glutathione peroxidase. Methods in enzymology: Elsevier;
372 1984. p.20-114 .
- 373 13. Habig WH, Pabst MJ, Jakoby WB. Glutathione S-transferases. J Biol Chem. 1974;249(22):7130-
374 9. doi:10.1016/S0021-9258(19)42083-8 .
- 375 14. Regoli F, Principato G. Glutathione, glutathione-dependent and antioxidant enzymes in mussel,
376 *Mytilus galloprovincialis*, exposed to metals under field and laboratory conditions: implications
377 for the use of biochemical biomarkers. Aquat Toxicol. 1995;31(2):143-64. doi:10.1016/0166-
378 445x(94)00064-w .
- 379 15. Weckbecker G, Cory JG. Ribonucleotide reductase activity and growth of glutathione-depleted
380 mouse leukemia L1210 cells *in vitro*. Cancer Lett. 1988;40(3):257-64. doi:10.1016/0304-
381 3835(88)90084-5 .

- 382 16. Draper HH, Hadley M. Malondialdehyde determination as index of lipid Peroxidation. Methods
383 in enzymology: Elsevier; 1990. p. 421-31..
- 384 17. Nadeem HR, Akhtar S, Sestili P, et al. Toxicity, Antioxidant Activity, and Phytochemicals of
385 Basil (*Ocimum basilicum* L.) Leaves Cultivated in Southern Punjab, Pakistan. Foods.
386 2022;11:1239. doi:10.3390/foods11091239.
- 387 18. Boulaares I, Derouiche S, Chetehouna S, Niemann J. *Ocimum basilicum* L. leaves extract-
388 mediated green synthesis of MnO NPs: Phytochemical profile, characterization, catalytic and
389 thrombolytic activities. Results in Surfaces and Interfaces. 2024;17:100284.
390 doi:10.1016/j.rsurfi.2024.100284.
- 391 19. Kumar V, Singh K, Panwar S, Mehta SK. Green synthesis of manganese oxide nanoparticles for
392 the electrochemical sensing of p-nitrophenol. Int Nano Lett. 2017;7:123-31. doi:10.1007/s40089-
393 017-0205-3.
- 394 20. Haschek WM, Rousseaux CG, Wallig MA. Chapter 5 - Techniques in Toxicologic Pathology.
395 Fundamentals of Toxicologic Pathology 2010. p. 81-92..
- 396 21. Zheng Q, Wang H, Hou W, Zhang Y. Use of anti-angiogenic drugs potentially associated with an
397 increase on serum AST, LDH, CK, and CK-MB activities in patients with cancer: a retrospective
398 study. Front cardiovasc med. 2021;8:755191. doi:10.3389/fcvm.2021.755191.
- 399 22. Medjdoub A, Merzouk S, Merzouk H, Chiali F, Narce M. Effects of Mancozeb and Metribuzin on
400 *in vitro* proliferative responses and oxidative stress of human and rat spleen lymphocytes
401 stimulated by mitogens. Pestic Biochem Physiol. 2011;101(1):27-33.
402 doi:10.1016/j.pestbp.2011.06.002.
- 403 23. Agarwal H, Nakara A, Shanmugam VK. Anti-inflammatory mechanism of various metal and
404 metal oxide nanoparticles synthesized using plant extracts: A review. Biomed Pharmacother.
405 2019;109:2561-72. doi:10.1016/j.biopha.2018.11.116.
- 406 24. Ilboudo S, Fouche E, Rizzati V, Toé AM, Gamet-Payrastre L, Guissou PI. In vitro impact of five
407 pesticides alone or in combination on human intestinal cell line Caco-2. Toxicol Rep. 2014;1:474-
408 89. doi:10.1016/j.toxrep.2014.07.008.
- 409 25. Boulaares I, Derouiche S, Niemann J. Greenly Synthesized Manganese Oxide Nanoparticles
410 (MnONPs) In Tumor Therapy? A Narrative Review. Arch Razi Inst. 2024.
411 doi:10.22092/ARI.2024.363798.2895.
- 412